Incorporating Diffuse Scattering in Geometry-based Stochastic MIMO Channel Models

J. Salmi*†, J. Poutanen†, K. Haneda†, A. Richter†, V.-M. Kolmonen†, P. Vainikainen†, A. F. Molisch*

*University of Southern California, Los Angeles, CA 90089-2565, United States
†Aalto University School of Science and Technology, P.O. Box 3000, FI-02015 Espoo, Finland
email: salmi@usc.edu

***Abstract*—This paper introduces a model for incorporating the influence of the diffuse scattering in the MIMO radio propagation channel to the popular geometry-based stochastic channel models (GSCM). The proposed model is based on a superposition of clusters, each of which contributes to the channel as a multivariate random variable having a Kronecker structured covariance matrix. These covariance matrices are derived based on parametric modeling of the angular and delay power spectral densities related to each cluster. The model also includes polarization and temporal evolution of the clusters. The proposed approach is validated using a spectral-based visual analysis comparing the model with measured channel sounding data.**

I. Introduction

Geometry-based Stochastic Channel Models (GSCM) [1]–[3] are a popular framework for modeling the radio propagation channel. These models are based on modeling the channel as a superposition of propagation paths obeying the plane wave assumption. The paths are grouped and parameterized in clusters, with each cluster representing a scattering object or a combination of objects defined by the geometry of the environment. The parameters of the clusters as well as the paths within the clusters can be drawn from scenario-dependent statistical distributions.

GSCM modeling is a very versatile approach for channel modeling. Due to the geometry-based approach, the dynamic properties, i.e., modeling the time evolution of the channel is inherently included. Moreover, one can define new scenarios and derive suitable parameters for them. However, existing channel models such as COST 259 [4], 3GPP SCM [5], COST 273 [2], Winner [3] neglect an important factor in radio wave propagation, namely the so-called dense multipath component (DMC). Each of the dominant propagation paths, i.e., the specular component (SC) of the radio channel, can be considered to convey individually significant signal power from the transmitter to the receiver. The DMC, on the other hand, results from diffuse scattering, i.e., it can be viewed as a superposition of (infinitely) many individually weak but dense scattering contributions. In other words, modeling the DMC using the propagation path model would require in principle infinitely many components. For example in [6] about 3000 path components were required to model only 70% of the power in measured small macrocellular channels. Neglecting the DMC also complicates the detection of some of the significant SC from measurements, see discussion in [7]. Furthermore, it has been shown in [8] that the contribution of the DMC to both the overall power in the channel as well MIMO channel capacity are very significant.

The first approach to include DMC in the GSCM was introduced in [9], where the DMC was modeled by a single exponentially decaying profile in delay, and was assumed to be uniformly distributed in the angular domain. However, the DMC can have a more complex behavior, exhibiting clustering, and existing predominantly in particular angular ranges. A main contribution of this paper is thus to propose a DMC model using a superposition of so called DMC clusters, which consider both delay and angular characteristics, as well as polarization. A further important aspect of this paper is to provide an efficient mechanism for incorporating such an advanced DMC model into the GSCM framework.

The remainder of the paper is organized as follows. Section II discusses the modeling of the radio propagation channel using SC and DMC. Section III introduces the proposed DMC model and its synthesis. Section IV provides comparison to measurements, and Section V concludes the paper.

II. Modeling Philosophy

A. Specular Paths vs. Diffuse Scattering

The model for the radio propagation channel is assumed to be comprised of two components: the specular component (SC), and the dense multipath component (DMC). Hence, the MIMO channel tensor $\mathcal{H} \in \mathbb{C}^{M_{MS} \times M_{BS} \times M_f \times M_k}$ can be written as

$$\mathcal{H} = \mathcal{H}_S + \mathcal{H}_D \tag{1}$$

where M_{MS}, M_{BS}, M_f, M_k denote the number of BS and MS antennas, frequency (delay) samples, and time (snapshot) samples, respectively. The SC ($\mathcal{H}_S$) is comprised of dominant propagation paths resulting from specular-like interactions such as reflections, whereas the DMC ($\mathcal{H}_D$) results from diffuse scattering present in all practical radio channels, see e.g. [10], [11], Table I.

The DMC is modeled as a multivariate zero-mean normal distributed random variable with specific correlation properties, hence yielding Rayleigh-like fading, whereas the SC is a superposition of deterministic propagation paths. It should be noted that the current GSCMs rely solely on SC for modeling

TABLE I
PROPERTIES OF SC VS. DMC.

Property	SC	DMC
Fading	N/A	Rayleigh
% of power indoors	10-50	50-90
% of power outdoors	20-80	20-80
Suitable representation	Discrete delta-functions	Continuous power distribution

the whole radio channel. The stochastic nature of SC comes from the fact that the SC parameters in GSCM are modeled as random variables.

B. Cluster-based Approach to DMC Modeling

Current GSCMs [2], [3] rely on modeling the channel as a superposition of propagation paths, i.e., the SC only. The paths are assumed to manifest themselves in clusters, i.e., groups of paths resulting from an interacting object of assumed geometrical position and statistical description. We propose to add DMC to this modeling concept by relating each, or some, of the clusters with a DMC component; an approach similar to the one proposed in [12]. The angular and delay parameters of the DMC should have correlation with those of the SC parameters, see [13]. This idea is illustrated in Fig. 1, where several types of clusters are identified:

- Near BS Cluster: Contributes to SC and/or DMC only,
- Near MS Cluster: Contributes to SC and/or DMC only,
- Far cluster(s): Contributes to SC only,
- Regular cluster(s): Contributes to SC and/or DMC only.

If a cluster includes both SC and DMC, it is reasonable to assume that the angular means, as well as the minimum delay, are equal for both SC and DMC. Also the spread parameters may be correlated.

III. PARAMETERIZATION AND SYNTHESIS OF THE DMC

The DMC is modeled as a complex valued, zero-mean, normal distributed, circular symmetric multivariate random variable $\mathrm{vec}\big(\mathcal{H}_D(t)\big) \sim \mathcal{N}_C(\mathbf{0}, \mathbf{R}_D(t))$. The DMC covariance matrix $\mathbf{R}_D(t)$ is modeled as a superposition of L DMC clusters as

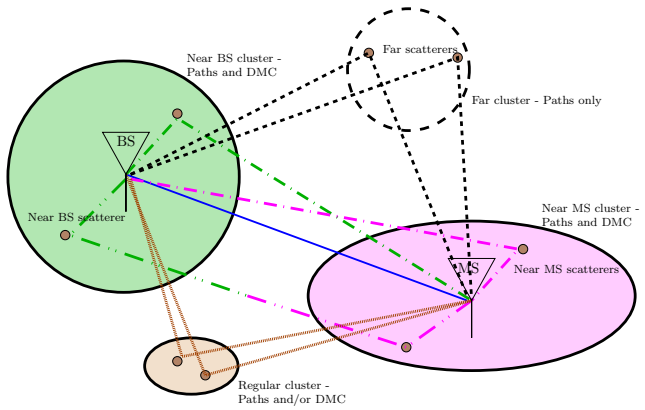

Fig. 1. GSCM principle including the DMC. The clusters may contribute either to the SC or the DMC only, or both.

$$\mathbf{R}_D(\boldsymbol{\theta}(t)) = \sum_{l=1}^{L} \mathbf{R}_f\left(\boldsymbol{\theta}_{f,l}(t)\right) \otimes \tag{2}$$
$$\Big[\, \gamma_{HH,l} \cdot \mathbf{R}_{MS,H}\left(\boldsymbol{\theta}_{MS,l}(t)\right) \otimes \mathbf{R}_{BS,H}\left(\boldsymbol{\theta}_{BS,l}(t)\right)$$
$$+\gamma_{HV,l} \cdot \mathbf{R}_{MS,H}\left(\boldsymbol{\theta}_{MS,l}(t)\right) \otimes \mathbf{R}_{BS,V}\left(\boldsymbol{\theta}_{BS,l}(t)\right)$$
$$+\gamma_{VH,l} \cdot \mathbf{R}_{MS,V}\left(\boldsymbol{\theta}_{MS,l}(t)\right) \otimes \mathbf{R}_{BS,H}\left(\boldsymbol{\theta}_{BS,l}(t)\right)$$
$$+\gamma_{VV,l} \cdot \mathbf{R}_{MS,V}\left(\boldsymbol{\theta}_{MS,l}(t)\right) \otimes \mathbf{R}_{BS,V}\left(\boldsymbol{\theta}_{BS,l}(t)\right) \,\Big],$$

where $\otimes$ denotes the Kronecker product, the coefficients $\gamma_{i,l}$, $i \in \{HH, HV, VH, VV\}$ denote the polarization[1] power ratios, with $\sum_i \gamma_{i,l} = 1$, and the vectors $\boldsymbol{\theta}$ contain the parameters describing the DMC. The matrices are normalized in such a way that each spatial covariance matrix $\mathbf{R}_{BS/MS,H/V}$ has unit norm. Hence, the overall DMC cluster power scale is determined by the matrix $\mathbf{R}_f$. The individual covariance matrices are modeled as follows.

A. Frequency Domain Covariance Matrix Model

The matrix $\mathbf{R}_f\left(\boldsymbol{\theta}_{f,l}\right)$ in (2) denotes the covariance matrix of the l^{th} cluster in frequency domain. Each cluster is modeled by an exponentially decaying delay profile. The frequency domain covariance matrices are thus given by [10]

$$\mathbf{R}_f\left(\boldsymbol{\theta}_{f,l}\right) = \mathrm{toep}\left(\boldsymbol{\lambda}(\boldsymbol{\theta}_{f,l}), \boldsymbol{\lambda}(\boldsymbol{\theta}_{f,l})^{\mathrm{H}}\right). \tag{3}$$

The operator $\mathrm{toep}(\bullet)$ denotes a Toeplitz matrix. The vector $\boldsymbol{\lambda}$ is a sampled version of the power spectral density, given by

$$\boldsymbol{\lambda}(\boldsymbol{\theta}_{f,l}) = \tag{4}$$
$$\frac{\alpha_{f,l}}{M_f}\left[\frac{1}{\beta_{f,l}} \;\; \frac{\mathrm{e}^{-\mathrm{j}2\pi\tau_{f,l}}}{\beta_{f,l} + \mathrm{j}2\pi\frac{1}{M_f}} \cdots \frac{\mathrm{e}^{-\mathrm{j}2\pi(M_f-1)\tau_{f,l}}}{\beta_{f,l} + \mathrm{j}2\pi\frac{M_f-1}{M_f}}\right]^{\mathrm{T}}.$$

Hence, the parameters of the frequency domain covariance matrix model are

$$\boldsymbol{\theta}_{f,l} = \left[\, \tau_{f,l} \;\; \alpha_{f,l} \;\; \beta_{f,l} \,\right]^{\mathrm{T}}, \tag{5}$$

where $\tau_{f,l}$ is the delay of arrival of the first component, $\alpha_{f,l}$ is the power of the first component, and $\beta_{f,l}$ is the normalized coherence bandwidth of the l^{th} DMC cluster.

B. Spatial Domain Covariance Matrix Model

The BS/MS covariance matrices in (2) are approximated for different polarizations (H/V) as

$$\mathbf{R}_{MS/BS,H/V}\left(\boldsymbol{\theta}_{MS/BS,l}\right) = \mathbf{B}_{MS/BS,H/V}\mathbf{K}(\boldsymbol{\theta}_{MS/BS,l})\mathbf{B}^{\mathrm{H}}_{MS/BS,H/V}, \tag{6}$$

where $\mathbf{B}_{MS/BS,H/V} \in \mathbb{C}^{M_{BS/MS} \times N_S}$ denotes a matrix of steering vectors at MS or BS for horizontal (H) or vertical (V) polarization evaluated at N_S directions defined in vectors $\boldsymbol{\varphi}_S$ and $\boldsymbol{\vartheta}_S$. The matrix $\mathbf{K}(\boldsymbol{\theta}_{MS/BS,l}) \in \mathbb{R}^{N_S \times N_S}$ is a diagonal matrix having the probability density values corresponding to the angles $\{\boldsymbol{\varphi}_S, \boldsymbol{\vartheta}_S\}$ on its diagonal. We propose a double

[1]HV is defined here as horizontal MS-vertical BS etc..

von Mises angular distribution, with individual mean and concentration parameter for both azimuth and elevation for each DMC cluster[2]. The matrix $\mathbf{K}(\boldsymbol{\theta}_{MS/BS,l})$ is defined as

$$\mathbf{K}(\boldsymbol{\theta}_{MS/BS,l}) = \\ \mathrm{diag}\big(\mathbf{f}_{\varphi}(\boldsymbol{\varphi}_S, \mu_{\varphi,l}, \kappa_{\varphi,l})\big)\mathrm{diag}\big(\mathbf{f}_{\vartheta}(\boldsymbol{\vartheta}_S, \mu_{\vartheta,l}, \kappa_{\vartheta,l})\big), \quad (7)$$

where the vectors $\mathbf{f}$ are the sampled von Mises angular distribution values, defined as

$$\Big\{\mathbf{f}(\boldsymbol{\theta}_S, \mu, \kappa)\Big\}_i = \frac{1}{2\pi I_0(\kappa)} \mathrm{e}^{\kappa\cdot\cos(\theta_{S,i}-\mu)}. \quad (8)$$

Hence, the parameters of a single cluster for the DMC model in the spatial domain are given by

$$\boldsymbol{\theta}_{MS} = [\ \mu_{\varphi,MS}\ \mu_{\vartheta,MS}\ \kappa_{\varphi,MS}\ \kappa_{\vartheta,MS}\ ]^{\mathrm{T}} \quad (9)$$

$$\boldsymbol{\theta}_{BS} = [\ \mu_{\varphi,BS}\ \mu_{\vartheta,BS}\ \kappa_{\varphi,BS}\ \kappa_{\vartheta,BS}\ ]^{\mathrm{T}} \quad (10)$$

$$\boldsymbol{\gamma} = [\ \gamma_{HH}\ \gamma_{HV}\ \gamma_{VH}\ \gamma_{VV}\ ]^{\mathrm{T}}, \quad (11)$$

and the overall DMC cluster parameters are given by (5), (9), (10), and (11) as

$$\boldsymbol{\theta} = \Big[\ \boldsymbol{\theta}_f^{\mathrm{T}}\ \boldsymbol{\theta}_{MS}^{\mathrm{T}}\ \boldsymbol{\theta}_{BS}^{\mathrm{T}}\ \boldsymbol{\gamma}^{\mathrm{T}}\ \Big]^{\mathrm{T}}. \quad (12)$$

As mentioned, each spatial covariance matrix (6) is normalized to have a unit norm, and $\sum_i \gamma_{i,l} = 1$.

C. Time evolution

The time evolution of the individual clusters at the channel realization level can be obtained using the autoregressive (AR) method described in [14]. This method is very suitable for the modeling of the multicluster DMC time evolution since the AR coefficients of the individual clusters can be adjusted over time according to the prevailing angular DMC cluster parameters and velocities. A n^{th} order AR process is obtained by the time domain recursion

$$x[k] = -\sum_{j=1}^{n} a_j x[k-j] + w[k], \quad (13)$$

where k is a discrete time index and $w[k]$ is a complex white Gaussian noise process with uncorrelated real and imaginary parts and variance σ_n^2. The filter coefficients $\{a_1, \ldots, a_n\}$ and the variance σ_n^2 can be determined based on the autocorrelation function (ACF).

The autocorrelation function (ACF), and its Fourier transform the Doppler power spectral density (DPSD), depend on the angular distribution and respective velocities of the transmitter, receiver, and cluster generating scatterers. For simplicity, we limit the discussion here to the case of a moving MS with isotropic antennas and single bounce scattering with von Mises angular distribution in azimuth only [15]. Description of a more general model can be found in [16]. The ACF for the l^{th} cluster depends on the MS velocity and the cluster's angular parameters, and is given by [14], [15]

$$r(k)(\kappa, \mu, f_m) = \\ \frac{I_0\left(\sqrt{\kappa^2 - (2\pi f_m|k|)^2 + j4\pi f_m|k|\kappa\cos(\mu)}\right)}{I_0(\kappa)} \quad (14)$$

where k is the discrete time snapshot index, $f_m = (f_c v/c)/f_s$ is the maximum Doppler frequency normalized by the snapshot sampling rate f_s, and $\kappa = \kappa_{\phi,MS,l}$ and $\mu = \mu_{\phi,MS,l}$ are the von Mises distribution parameters. Given the ACF (14), the AR coefficients $\mathbf{a} = [a_1\ \cdots\ a_n]^{\mathrm{T}}$ can be solved as

$$\mathbf{a} = -\widehat{\mathbf{R}}_{rr}^{-1}\mathbf{v}, \quad (15)$$

$$\widehat{\mathbf{R}}_{rr} = \mathrm{toep}\left([r(0)\ \cdots\ r(n-1)]^{\mathrm{T}}, [r(0)\ \cdots\ r(n-1)]^{*}\right) + \epsilon\mathbf{I},$$

$$\mathbf{v} = [r(1)\ \cdots\ r(n)]^{\mathrm{T}}.$$

The small spectral bias ϵ improves the stability of solving (15) by increasing the condition number of $\widehat{\mathbf{R}}_{rr}$. The variance σ_n^2 of the process is given by

$$\sigma_n^2 = r(0) + \sum_{j=1}^{n} a_j r(j)^*. \quad (16)$$

Discussion on the stability conditions and initialization of the process can be found in [14].

D. Synthesis

The proposed cluster-based DMC extension to GSCM can be synthesized as follows. First, the time evolution for each of the l clusters is established by generating n (n is the AR model order in (13)) samples $\mathcal{H}_{d,l}(k) \in \mathbb{C}^{M_{BS}\times M_{MS}\times M_f}$ for $k = \{-n, \ldots, -1\}$ using the initialization method described in [14]. Then for each snapshot $k = \{0, \ldots, K\}$ i) a new realization $\mathcal{H}_{d,l}(k)$ is drawn based on the cluster parameter based AR model of each cluster l, and ii) the covariance matrices (3) and (6) are computed. A complete DMC realization is constructed as

$$\mathrm{vec}\big(\mathcal{H}_D(k)\big) = \mathrm{vec}\Big(\sum_{l=1}^{L}\Big(\mathbf{R}_{MSBS,l}^{\frac{1}{2}}\mathbf{H}_{d,l}(k)(\mathbf{R}_{f,l}^{\frac{1}{2}})^{\mathbf{T}}\Big)\Big), \quad (17)$$

where $\mathbf{H}_{d,l}(k) \in \mathbb{C}^{M_{MS}M_{BS}\times M_f}$ denotes $\mathcal{H}_{d,l}(k)$ reshaped into a matrix, and

$$\mathbf{R}_{MSBS,l} = \sum_{pol} \gamma_{polpol,l}\mathbf{R}_{MS,pol,l} \otimes \mathbf{R}_{BS,pol,l}. \quad (18)$$

IV. Comparison to Measurement Results

This section provides a comparison of the proposed model to a real-world propagation channel realization obtained from a MIMO channel sounding measurement. A map of the measurement venue as well as the BS/MS locations are shown in Fig. 2a. The BS was located at the edge of a large open space separating two corridors with offices and classrooms along them. The MS was moved across the center of the open space along a bridge connecting the two corridors. Measurements were conducted with a 120 MHz bandwidth at 5.3 GHz

[2]It should be mentioned that double von Mises distribution model is valid only if the elevation angles are somewhat concentrated on the vicinity of the equator of the unit sphere.

carrier frequency. The antenna arrays at both link ends support high resolution directional and polarization analysis. The same measurement has been analyzed for the SC clusters in [17]. Fig. 2b shows the Power–BS azimuth–MS azimuth–Profile (PAAP) for the complete measured channel $\mathcal{H}$ in (1), as well as the residual (DMC) channel $\widehat{\mathcal{H}}_D = \mathcal{H} - \widehat{\mathcal{H}}_S$. The SC are estimated using propagation path parameter estimates obtained by the EKF algorithm [11]. The plots in Fig. 2b (and Fig. 3) are obtained by Bartlett beamforming in the azimuth plane at both link ends using orthogonal polarization responses, and the results are averaged over the delay domain. Fig. 2b represents the sum power of the different polarization components of a single snapshot. It can be observed that the DMC contains a significant contribution to the channel.

Fig. 3 shows a comparison of the DMC PAAP (see Fig. 2b) separately for different polarization components between the measured and modeled DMC channel. Note that the color scale is different than in Fig. 2b. The modeled DMC data in Fig. 3b are constructed with (17) using 10 DMC clusters. The parameters of the DMC clusters are determined visually based on the measurement data in Fig. 3a and Fig. 4a. Some of the key parameters are listed in Table II. The following parameters were fixed for all clusters to simplify the analysis based on visual inspection: $\mu_{\vartheta,MS} = \mu_{\vartheta,BS} = 0°$, $\kappa_{\vartheta,MS} = \kappa_{\vartheta,BS} = 10$, $\beta_f = 0.12$. Cluster #10 has $\kappa_{\varphi,BS} = \kappa_{\varphi,MS} = 0$, i.e., a uniform pdf in azimuth, corresponding to local scattering around both terminals. For other clusters the azimuth spread parameter of the von Mises distribution varies between 5 and 50 and the cluster powers α_f were given values ranging from -43 dB to -38 dB.

Fig. 4 compares the measured DMC data with the 10-cluster DMC model through Power–Azimuth–Delay–Profiles (PADP).

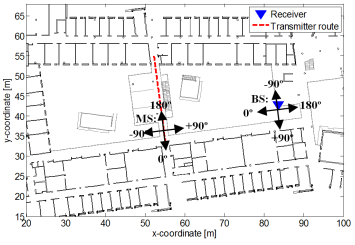

(a) Map of the measurement venue.

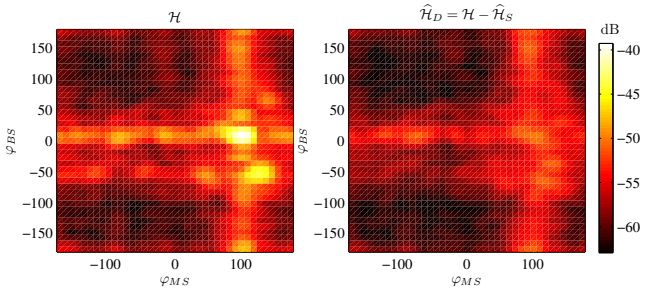

(b) Map of the measurement venue.

Fig. 2. Map of the measurement venue and the Power–BS azimuth–MS azimuth–Profile of the complete measured channel $\mathcal{H}$ as well as the residual (DMC) channel after removing SC $\mathcal{H}_D = \mathcal{H} - \mathcal{H}_S$.

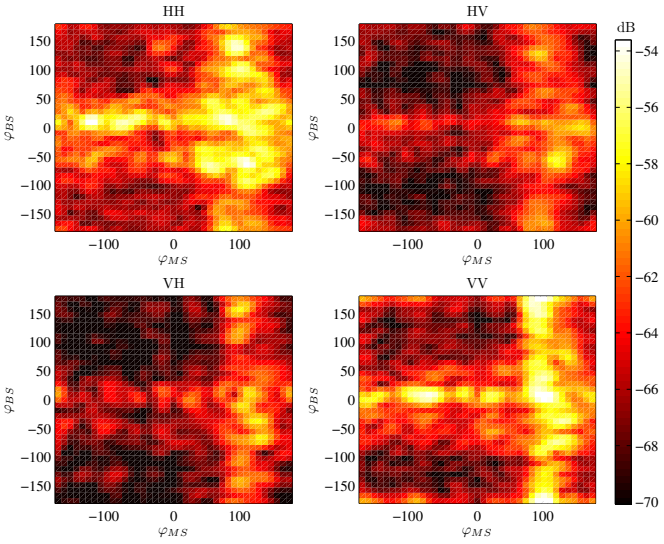

(a) Measured DMC.

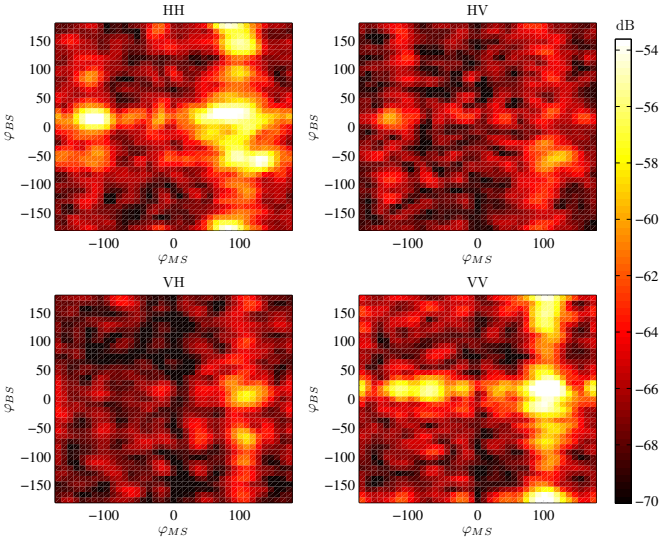

(b) Modeled DMC.

Fig. 3. Comparison of measured and modeled DMC Power–BS azimuth–MS azimuth-Profile for different (HH, HV, VH, VV) polarization components.

The plots are given for different polarization responses at the corresponding link end, i.e., V-pol for MS contains both VV and VH polarization components, etc..

The visual comparison of the measured and modeled responses in Fig. 4 and Fig. 3 show that the model provides means to accurately characterize the MIMO propagation channel in terms of directional, delay, and polarization properties. Much higher accuracy can be expected if all the parameters are jointly optimized by a sophisticated estimation algorithm.

TABLE II
SELECTED DMC CLUSTER PARAMETERS.

#	1	2	3	4	5	6	7	8	9	10
τ_f (ns)	120	160	120	160	155	150	165	250	150	120
$\mu_{\varphi,BS}$	10°	10°	5°	5°	180°	180°	140°	140°	-60°	N/A
$\mu_{\varphi,MS}$	-125°	-80°	100°	80°	100°	80°	100°	100°	110°	N/A
Pol	HH/HV	VV	VV/VH	HH	VV	HH	VV	HH	HH/HV	ALL

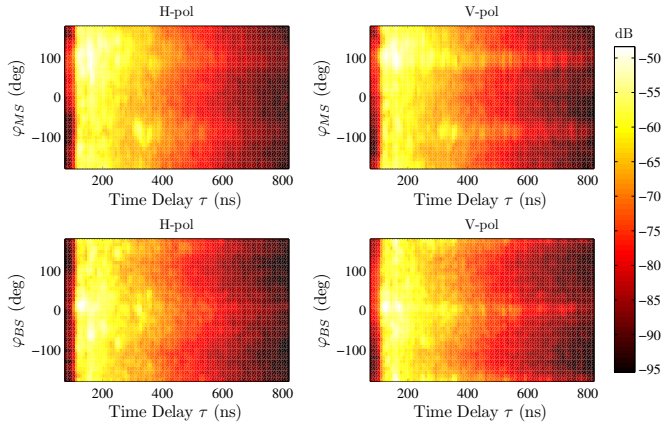

(a) Measured.

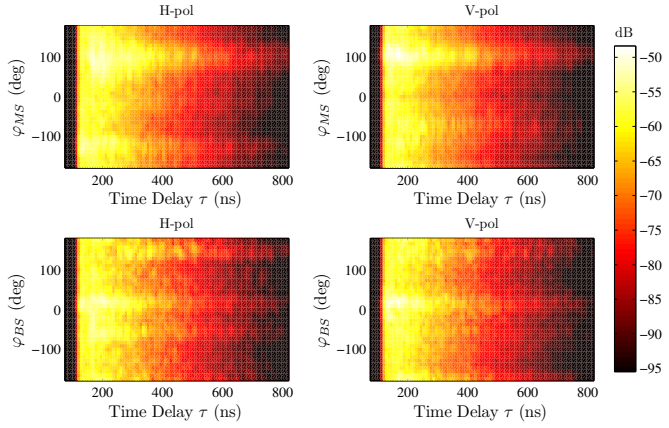

(b) Modeled.

Fig. 4. Comparison of measured and modeled Power–Azimuth–Delay–Profiles for horizontal and vertical polarizations observed at both link ends.

V. Conclusions

The proposed cluster-based DMC model can be applied to extend current geometry based stochastic channel models. The proposed cluster-wise, Kronecker structured, multivariate random variable model describes the DMC contribution of the channel through the power spectral densities of each cluster in the angular and delay domain. The model also enables polarization and time-evolution modeling. Comparison to measured MIMO channel sounding data shows that the proposed model can be used to capture the diffuse part of the channel, which is hard to estimate using discrete propagation paths. Potential future work includes deriving i) an estimator for the model parameters, ii) a scheme for finding the correct number of DMC clusters and their initial parameters, iii) the correlation between DMC and SC clusters, iv) proper model for describing the angular distribution of the DMC clusters on the sphere. Also, comparison of different models (SC only, SC + uniform DMC) using different metrics, such as channel capacity, is of high practical interest.

Acknowledgements

This research was partially conducted within the Nordite WILATI project. The first author would like to thank Academy of Finland, Technology Promotion Foundation (TES), and Walther Ahlström foundation for financial support. The efforts of Peter Almers and Jukka Koivunen in participating in the measurements are also acknowledged.

References

[1] J. Fuhl, A. Molisch, and E. Bonek, "Unified channel model for mobile radio systems with smart antennas," *IEE Proceedings – Radar, Sonar and Navigation*, vol. 145, no. 1, pp. 32–41, Feb. 1998.

[2] L. M. Correia, Ed., *Mobile Broadband Multimedia Networks*, 1st ed. Academic Press, May 2006, 608 p.

[3] P. Kyösti, J. Meinilä, L. Hentilä, X. Zhao, T. Jämsä, C. Schneider, M. Narandzić, M. Milojević, A. Hong, J. Ylitalo, V.-M. Holappa, M. Alatossava, R. Bultitude, Y. de Jong, and T. Rautiainen, "WINNER II channel models," IST-WINNER, Deliverable D1.1.2, 2007. [Online]. Available: http://www.ist-winner.org/WINNER2-Deliverables/D1.1.2v1.1.pdf

[4] A. Molisch, H. Asplund, R. Heddergott, M. Steinbauer, and T. Zwick, "The COST 259 directional channel model-part I: Overview and methodology," *IEEE Transactions on Wireless Communications*, vol. 5, no. 12, pp. 3421–3433, Dec. 2006.

[5] G. Calcev, D. Chizhik, B. Goransson, S. Howard, H. Huang, A. Kogiantis, A. Molisch, A. Moustakas, D. Reed, and H. Xu, "A wideband spatial channel model for system-wide simulations," *IEEE Transactions on Vehicular Technology*, vol. 56, no. 2, pp. 389–403, Mar. 2007.

[6] J. Medbo, M. Riback, H. Asplund, and J. Berg, "MIMO channel characteristics in a small macrocell measured at 5.25 GHz and 200 MHz bandwidth," in *The 62nd IEEE VTC 2005-Fall*, vol. 1, Dallas, TX, Sept., 2005, pp. 372–376.

[7] G. Steinböck, J.-M. Conrat, T. Pedersen, and B. H. Fleury, "On initialization and search procedures for iterative highresolution channel parameter estimators," *COST2100 9th Management Committee Meeting*, Vienna, Austria, TD(09)956, Sept. 28–30, 2009.

[8] A. Richter, J. Salmi, and V. Koivunen, "On distributed scattering in radio channels and its contribution to MIMO channel capacity," in *The 1st European Conference on Antennas and Propagation (EuCAP 2006)*, Nice, France, Nov. 2006, pp. 1–7.

[9] N. Czink, A. Richter, E. Bonek, J.-P. Nuutinen, and J. Ylitalo, "Including diffuse multipath parameters in MIMO channel models," in *The 66th IEEE VTC 2007-fall*, Baltimore, MD, Sept. 2007.

[10] A. Richter, "Estimation of radio channel parameters: Models and algorithms," Ph. D. dissertation, Technischen Universität Ilmenau, Germany, May 2005, ISBN 3-938843-02-0. [Online]. Available: www.db-thueringen.de

[11] J. Salmi, "Contributions to measeurement-based dynamic MIMO channel modeling and propagation parameter estimation," Ph. D. dissertation, Helsinki University of Technology, Dept. of Signal Processing and Acoustics, Espoo, Finland, Aug. 2009, report 10, ISBN: 978-952-248-018-7. [Online]. Available: http://lib.tkk.fi/Diss/2009/isbn9789522480194/

[12] J. Kunisch and J. Pamp, "An ultra-wideband space-variant multipath indoor radio channel model," in *IEEE Conference on Ultra Wideband Systems and Technologies*, Reston, VA, Nov. 2003, pp. 290–294.

[13] J. Poutanen, K. Haneda, J. Salmi, V.-M. Kolmonen, and P. Vainikainen, "Angular characteristics of dense multipath components in indoor radio channels," *COST2100 9th Management Committee Meeting*, Vienna, Austria, TD(09)911, Sept. 28–30, 2009.

[14] K. Baddour and N. Beaulieu, "Autoregressive modeling for fading channel simulation," *IEEE Transactions on Wireless Communications*, vol. 4, no. 4, pp. 1650–1662, July 2005.

[15] A. Abdi, J. Barger, and M. Kaveh, "A parametric model for the distribution of the angle of arrival and the associated correlation function and power spectrum at the mobile station," *IEEE Transactions on Vehicular Technology*, vol. 51, no. 3, pp. 425–434, May 2002.

[16] A. Zajic and G. Stubber, "Space-time correlated mobile-to-mobile channels: Modelling and simulation," *IEEE Transactions on Vehicular Technology*, vol. 57, no. 2, pp. 715–726, Mar. 2008.

[17] J. Poutanen, K. Haneda, J. Salmi, V.-M. Kolmonen, F. Tufvesson, and P. Vainikainen, "Analysis of radio wave scattering processes for indoor MIMO channel models," in *The 20th Personal Indoor and Mobile Radio Communications Symposium (PIMRC09)*, Tokyo, Japan, Sept. 13–16 2009.